NATIONAL ADVISORY COMMITTEE FOR AERONAUTICS

TECHNICAL NOTE 4117

EXPERIMENTAL INVESTIGATION OF LIFT, DRAG, AND PITCHING MOMENT OF FIVE ANNULAR AIRFOILS

By Herman S. Fletcher

Langley Aeronautical Laboratory
Langley Field, Va.

Washington
October 1957

1F

NATIONAL ADVISORY COMMITTEE FOR AERONAUTICS

TECHNICAL NOTE 4117

EXPERIMENTAL INVESTIGATION OF LIFT, DRAG, AND PITCHING MOMENT OF FIVE ANNULAR AIRFOILS

By Herman S. Fletcher

SUMMARY

An investigation was carried out in the Langley stability tunnel to determine the lift, drag, and pitching-moment characteristics of a family of annular airfoils. The five annular airfoils had equal projected areas but had varying chords and diameters which covered aspect ratios of 1/3, 2/3, 1.0, 1.5, and 3.0.

The results showed that the effects of aspect ratio on the aerodynamic-center location were similar for annular and unswept airfoils and that annular airfoils had larger maximum lift-drag ratios below an aspect ratio of 2.4 than did plane rectangular airfoils with faired tips. The lift-curve slope was twice the lift-curve slope for a plane unswept airfoil of the same aspect ratio, and the induced drag coefficient was one-half the induced drag coefficient of an elliptic airfoil. The characteristics of the flow in the wake of the annular airfoils having lower aspect ratios (1/3, 2/3, and 1.0) were similar to the wake characteristics of low-aspect-ratio or highly swept airfoils.

INTRODUCTION

Considerable interest has been shown recently in the aerodynamic characteristics of annular airfoils and the application of the annular airfoil as the primary lifting surface to such configurations as vertical-take-off aircraft (refs. 1 and 2) and one-man vertically rising aircraft (ref. 3).

Reference 4 presents low-speed static-longitudinal-stability data for annular airfoils of aspect ratios 1.56 and 2.5 (the aspect ratio is equal to the diameter divided by the chord). Lift-coefficient data are also presented for a wing-body combination with annular airfoils of aspect ratios 1.56 and 2.5 at supersonic speeds. Additional low-speed data are available in reference 3 on an annular shroud (annular wing with flat-plate section) of aspect ratio 1.47. However, aerodynamic data on annular airfoils of very low aspect ratios (1/3, 2/3, and 1.0), as well as data for an aspect ratio of 3.0, appear to be lacking.

Therefore, the purpose of this investigation was to provide data on the low-speed static longitudinal stability characteristics of a family of annular airfoils that covered a wider range of aspect ratios than those found in references 3 and 4. The family of annular airfoils tested in this investigation had equal projected areas, but varying chords and diameters. The variation of chords and diameters covered aspect ratios of 1/3, 2/3, 1.0, 1.5, and 3.0.

SYMBOLS AND COEFFICIENTS

The data presented herein are referred to the system of axes shown in figure 1. The forces and moments were measured at and about the quarter-chord (fig. 2). The symbols and coefficients are defined as follows:

A	aspect ratio, d/c
S	projected area of annular airfoil, dc, sq ft
d	inner diameter, ft
c	chord parallel to center line of annular airfoil, ft
q	dynamic pressure, $\frac{\rho}{2}V^2$, lb/sq ft
ρ	mass density of air, slugs/cu ft
V	airspeed, ft/sec
α	angle of attack of center line of annular airfoil, deg
C_L	lift coefficient, Lift/qS
C_D	drag coefficient, Drag/qS
$C_{D,o}$	drag coefficient at $\alpha = 0^o$
C_m	pitching-moment coefficient, Pitching moment/qSc
C_{L_α}	lift-curve slope per degree
a	section lift-curve slope, per radian
x_{cp}	location of center of pressure in percent chord from leading edge

x_{ac} location of aerodynamic center in percent chord from leading edge

L/D lift-drag ratio

x tuft-grid position downstream of wing trailing edge, in.

MODELS AND APPARATUS

The models used in this investigation were constructed of laminated mahogany and consisted of five annular airfoils having equal projected areas (S = Diameter × Chord), but varying chords and diameters (fig. 2). The variation of chords and diameters covered aspect ratios of 1/3, 2/3, 1.0, 1.5, and 3.0. The annular airfoils had Clark Y airfoil sections with a maximum thickness ratio of 0.117.

The tests of this investigation were made in the 6- by 6-foot test section of the Langley stability tunnel. For the force tests, the models were mounted on a single support strut which was rigidly attached to a six-component electromechanical balance system. The height of the support strut was varied in order to mount the center lines of the various models on the center of the balance system. All the models were mounted at their respective quarter-chord points. For the tuft-grid tests, the models were mounted on a horizontal wire and held at the desired angle of attack by additional wires attached to the leading and trailing edges of the airfoil.

TESTS

The force tests were made at a dynamic pressure of 24.9 pounds per square foot, which corresponds to a Mach number of 0.13. The Reynolds numbers based on the respective chords of each annular airfoil varied from 0.704×10^6 to 2.11×10^6. The models were tested throughout an angle-of-attack range from about -4° to 90°. Additional tests were made with a tuft grid located in two positions. The initial position was as close as was practical (1.5 to 6.0 inches) behind the trailing edge, and the second position was 24 inches downstream from the initial position. For the tuft-grid tests the models were placed at an angle of attack approximately 4° below the stall for each airfoil, and the tests were made at a dynamic pressure of 8 pounds per square foot.

CORRECTIONS

Approximate jet-boundary corrections (ref. 5) were applied to the angle of attack and to the drag coefficient. Blockage corrections were considered to be negligible and hence were not applied. Tare corrections for the support-strut interference were determined for each model and applied to the data.

RESULTS AND DISCUSSION

The basic data of this investigation are presented as the variation of C_L, C_D, and C_m with α in figures 4 to 6. Each figure covers the range of aspect ratios. The lift-coefficient data for the smallest aspect ratios did not show the characteristic nonlinearity of low-aspect-ratio rectangular wings below the stall. For aspect ratios of 1.5 and 3.0 the abruptness of the force break agreed well with the data of reference 6 for the wings with the faired tips. For aspect ratios below 1.5, however, the force break was fairly smooth with none of the sharp losses of lift above 45° and 50° shown in reference 6 for aspect ratios of 0.90 and 0.65, respectively.

The pitching-moment data were used to determine the center-of-pressure locations for each angle of attack, and this information is presented in figure 7. For all airfoils except the one having the lowest aspect ratio (1/3), the center of pressure was fairly constant throughout most of the unstalled angle-of-attack range. At the stall, the center of pressure moved to a more rearward position that also remained nearly constant throughout the remainder of the angle-of-attack range. For the airfoil having an aspect ratio of 1/3, however, the center of pressure shifted rearward with increasing angle of attack (similar to the center-of-pressure movement on a slender body of revolution) throughout the angle-of-attack range. The flow about the annular airfoils having very low aspect ratios appears to have some of the characteristics of the flow about inclined solid bodies of revolution. (See ref. 7.)

Figure 8 shows the location of the aerodynamic center of the annular airfoil measured at angles of attack between 0° and 10° as a function of aspect ratio. The aerodynamic center moves rearward with increase in aspect ratio. In this respect, the effects of aspect ratio on the aerodynamic center are similar to the effects of aspect ratio on the aerodynamic center for a plane wing (ref. 8). The aerodynamic center of the annular airfoil having an aspect ratio of 1/3 is located ahead of the wing leading edge. This annular airfoil is more like a slender body of revolution (similar to a fuselage) than any of the annular airfoils having higher aspect ratios and would thus be expected to exhibit the unstable pitching-moment characteristics as well as the low lift of slender bodies of revolution.

Figure 9 shows lift-drag ratio plotted against angle of attack. The curves are nearly alike for all wings at angles of attack above 35°. At angles of attack between 0° and 35°, however, the curves become flatter with decrease in aspect ratio, but the peaks of the curves are not so rounded and smooth as the curves of L/D of reference 6 for the wings with the faired tips. These sharp peaks may indicate a more unstable aerodynamic condition near the stall for the annular airfoils than for low-aspect-ratio wings. Figure 10 is a comparison of the maximum values of L/D obtained for the annular airfoils and the maximum values of L/D obtained for the faired-tip airfoils of reference 6. The annular airfoils have larger values of maximum L/D and hence smaller minimum glide angles below an aspect ratio of 2.4 than the plane faired-tip airfoils of reference 6.

Figure 11 presents a comparison of the experimental and calculated lift-curve slopes. Lift-curve slopes (curve A) estimated by the high-aspect-ratio theory of reference 9 in which the experimental section-lift-curve slope (ref. 10) was used instead of 2π are in good agreement with the experimental lift-curve slopes for aspect ratios above 2.4. This result was obtained by the application of lifting-line theory to the annular airfoil problem. The lift-curve slopes (curve B) calculated by the low-aspect-ratio annular-airfoil theory of reference 9 are in good agreement with the experimental lift-curve slopes for aspect ratios less than 1.

Reference 9 also indicated as a general conclusion that the lift of an annular airfoil is twice the lift of an elliptic flat plate that spans the diameter and has one-quarter the area of the annular airfoil. The result obtained by applying this conclusion and using accurate theoretical values for the lift of an elliptic wing obtained from reference 8 rather than using lifting-line theory as a basis is shown by curve C of figure 11. This procedure gives good agreement with the experimental results throughout the aspect-ratio range of these tests.

Curve D of figure 11 represents the lift-curve slopes obtained by simply doubling the lift-curve slope of a rectangular plane wing (ref. 8) that spans the diameter of the annular airfoil. The agreement between this result and experiment is also good.

Reference 4 indicates that the induced drag coefficient of an annular airfoil can be computed from $C_L^2/2\pi A$, which is one-half the induced drag of an elliptic wing. The use of this result as a basis for calculating the induced drag coefficient from the lift coefficients gave values that were in good agreement with the experimental values (fig. 12).

The tuft-grid photographs of the wake characteristics at two positions behind the annular airfoils are presented in figure 13. In general,

the photographs show that the flow characteristics behind the annular airfoils having lower aspect ratios (1/3, 2/3, and 1.0) were similar in nature to the flow characteristics behind low-aspect-ratio or highly swept plane airfoils (ref. 11). Two vortices can be seen to emanate from the trailing edge of the annular airfoil and move downstream in a manner similar to the vortices shed from a plane airfoil. There is some lateral inward movement as well as a distinct downward movement of the vortices as they move on downstream in a manner similar to the vortices shed by highly swept wings. At the higher aspect ratios (1.5 and 3.0), the vortices appear to move very little if any laterally or downward as they pass on downstream in a manner very similar to the vortices shed by unswept wings (ref. 11). The presence of a distributed vortex sheet may be noted for the close position of the tuft grid. This sheet rolls up into two discrete vortices by the time that the wake reaches the rearmost positions.

CONCLUSIONS

The results of an investigation made in the Langley stability tunnel to determine the aerodynamic characteristics of a family of annular airfoils indicated the following conclusions:

1. The effects of aspect ratio on the aerodynamic-center location of the annular airfoil were similar to the effects of aspect ratio on the aerodynamic-center location for a plane unswept airfoil.

2. The annular airfoils had larger maximum lift-drag ratios below an aspect ratio of 2.4 than did plane unswept airfoils with faired tips.

3. The lift-curve slopes of the annular airfoils were approximately twice the lift-curve slopes for a plane rectangular airfoil having the same aspect ratio.

4. The induced drag coefficient of the annular airfoil was one-half the induced drag coefficient of an elliptic airfoil.

5. For the annular airfoils having lower aspect ratios (1/3, 2/3, and 1.0) the flow characteristics in the wake were similar in nature to the flow characteristics in the wake of low-aspect-ratio or highly swept plane wings.

Langley Aeronautical Laboratory,
National Advisory Committee for Aeronautics,
Langley Field, Va., July 11, 1957.

REFERENCES

1. Bergaust, Erik: The Coleopter - World's Most Radical Aircraft. Aero. Digest, vol. 70, no. 6, June 1955, pp. 22-25.

2. Weyl, A. R.: Coleopter Combines Wing and Powerplant. Aviation Age, vol. 24, no. 5, Nov. 1955, pp. 32-37.

3. Parlett, Lysle P.: Aerodynamic Characteristics of a Small-Scale Shrouded Propeller at Angles of Attack From 0° to 90°. NACA TN 3547, 1955.

4. Plaskowski, Z.: Annular Airfoils. Report presented to Fourth Int. Astronautical Congress (Zurich), Laubscher Cie (Biel-Bienne, Switzerland), Aug. 5, 1953.

5. Silverstein, Abe, and White, James A.: Wind-Tunnel Interference With Particular Reference to Off-Center Positions of the Wing and to the Downwash at the Tail. NACA Rep. 547, 1936.

6. Zimmerman, C. H.: Characteristics of Clark Y Airfoils of Small Aspect Ratios. NACA Rep. 431, 1932.

7. Allen, H. Julian, and Perkins, Edward W.: A Study of Effects of Viscosity on Flow Over Slender Inclined Bodies of Revolution. NACA Rep. 1048, 1951.

8. DeYoung, John: Theoretical Additional Span Loading Characteristics of Wings With Arbitrary Sweep, Aspect Ratio, and Taper Ratio. NACA TN 1491, 1947.

9. Ribner, Herbert S.: The Ring Airfoil in Nonaxial Flow. Jour. Aero. Sci., vol. 14, no. 9, Sept. 1947, pp. 529-530.

10. Jacobs, Eastman N., and Abbott, Ira H.: Airfoil Section Data Obtained in the N.A.C.A. Variable-Density Tunnel As Affected by Support Interference and Other Corrections. NACA Rep. 669, 1939.

11. Bird, John D., and Riley, Donald R.: Some Experiments on Visualization of Flow Fields Behind Low-Aspect-Ratio Wings by Means of a Tuft Grid. NACA TN 2674, 1952.

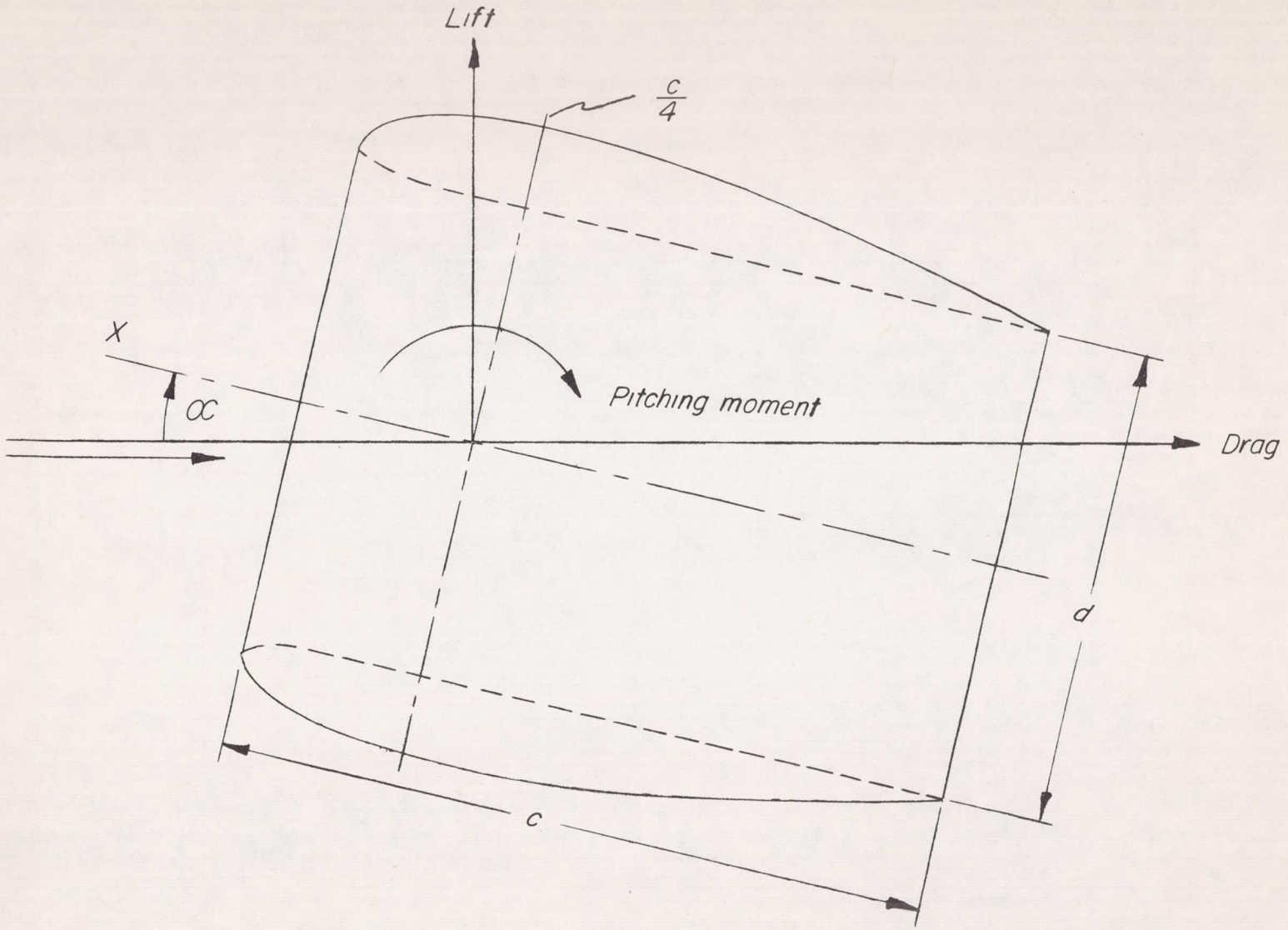

Figure 1.- System of axes employed in annular airfoil tests. Arrows indicate positive directions of forces, moments, and displacements.

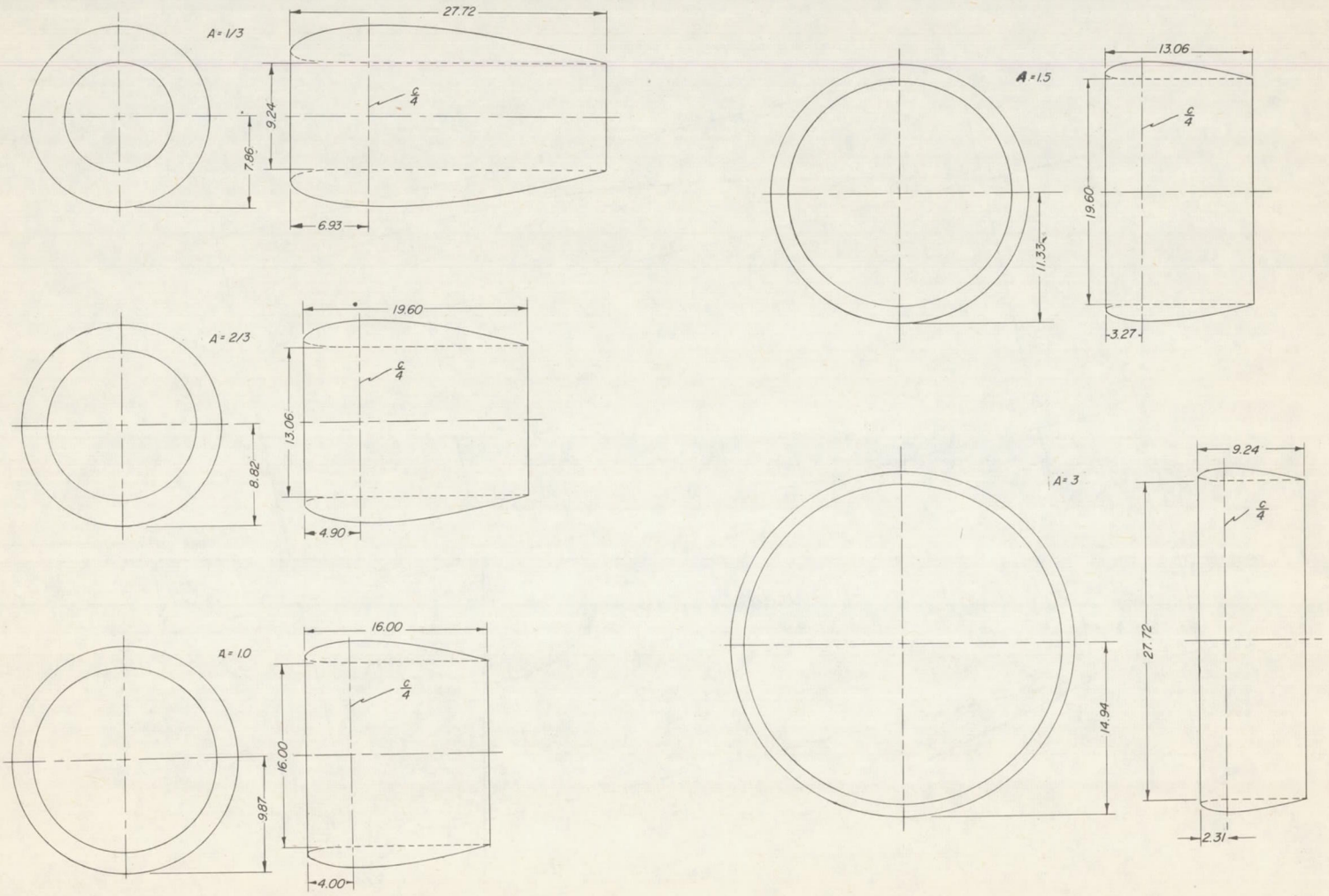

Figure 2.- Models used in investigation. All dimensions are in inches.

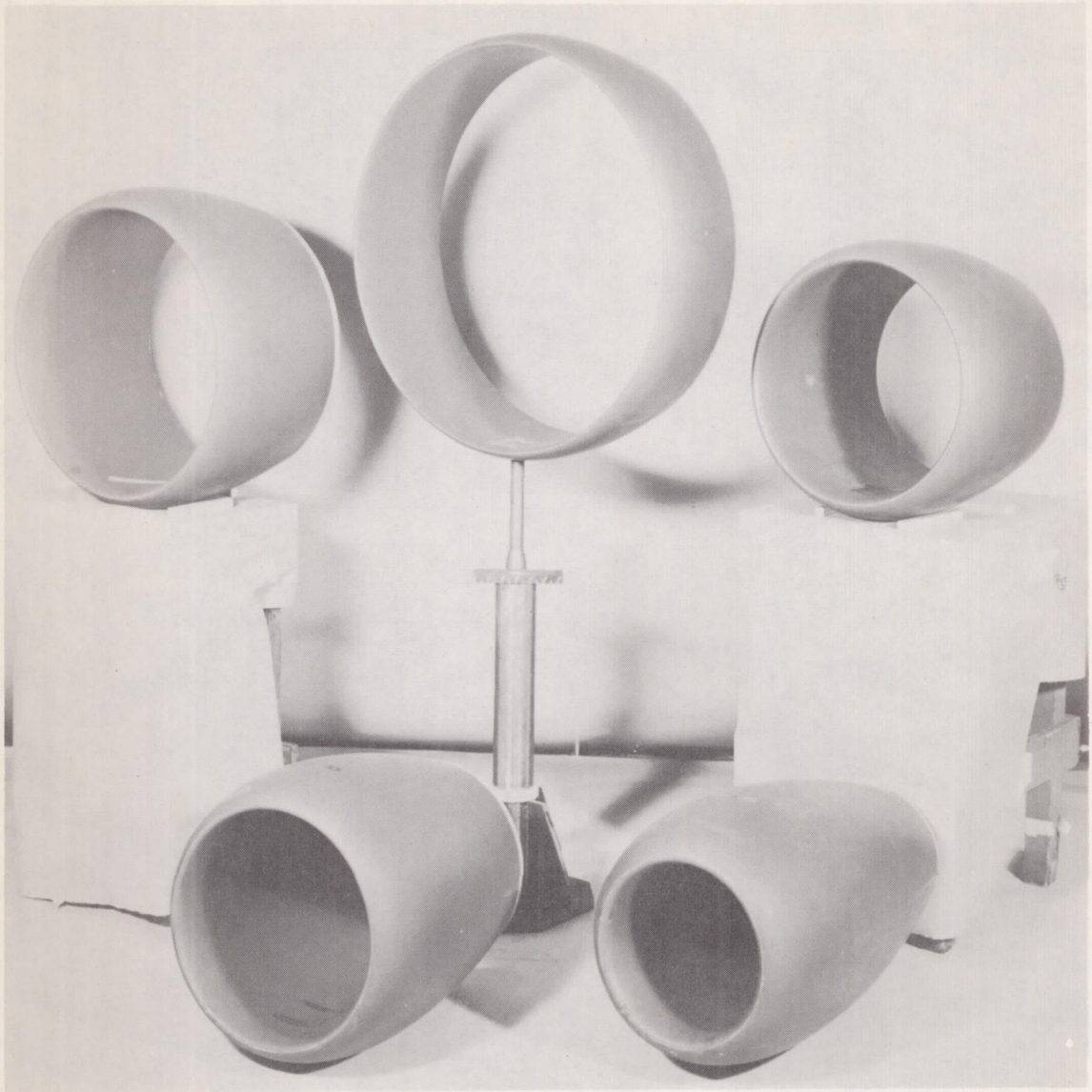

Figure 3.- Models tested in this investigation. L-57-66

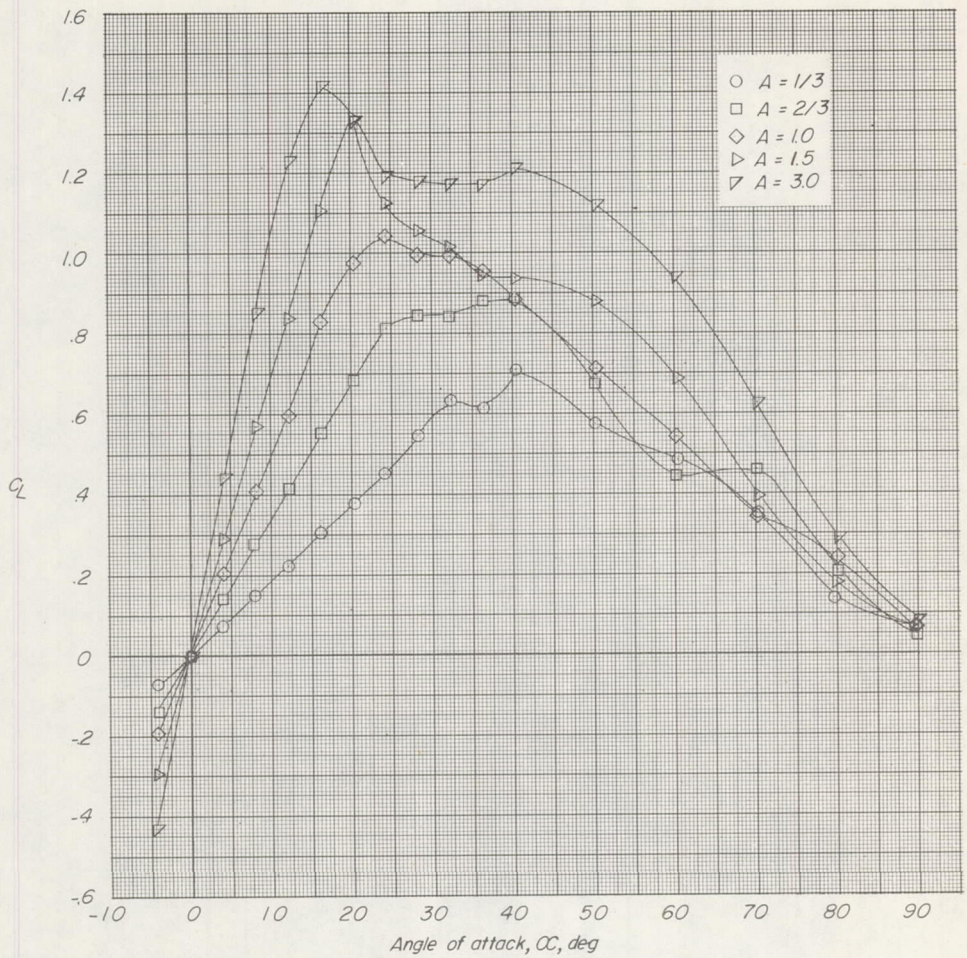

Figure 4.- Variation of lift coefficient with angle of attack for various aspect ratios.

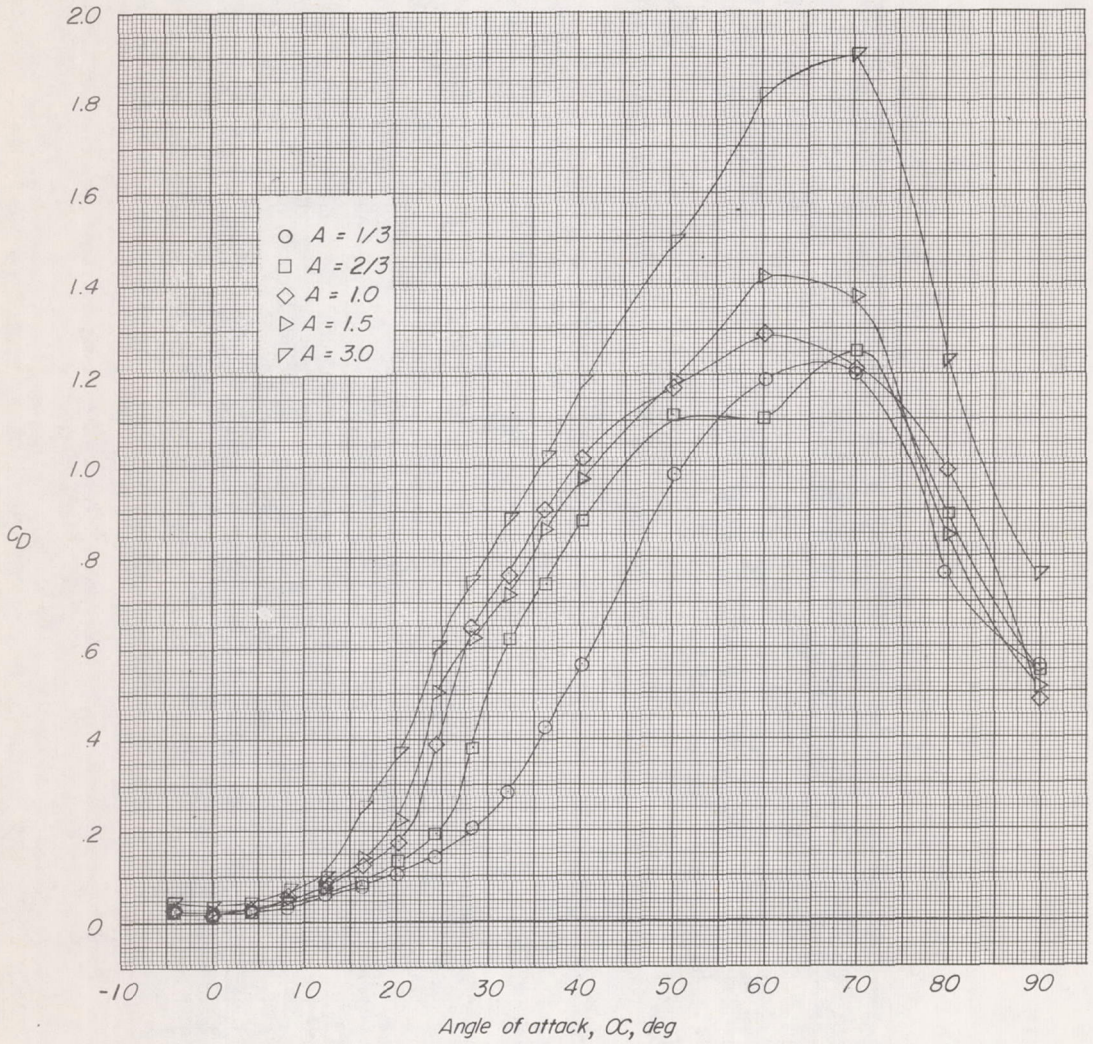

Figure 5.- Variation of drag coefficient with angle of attack for various aspect ratios.

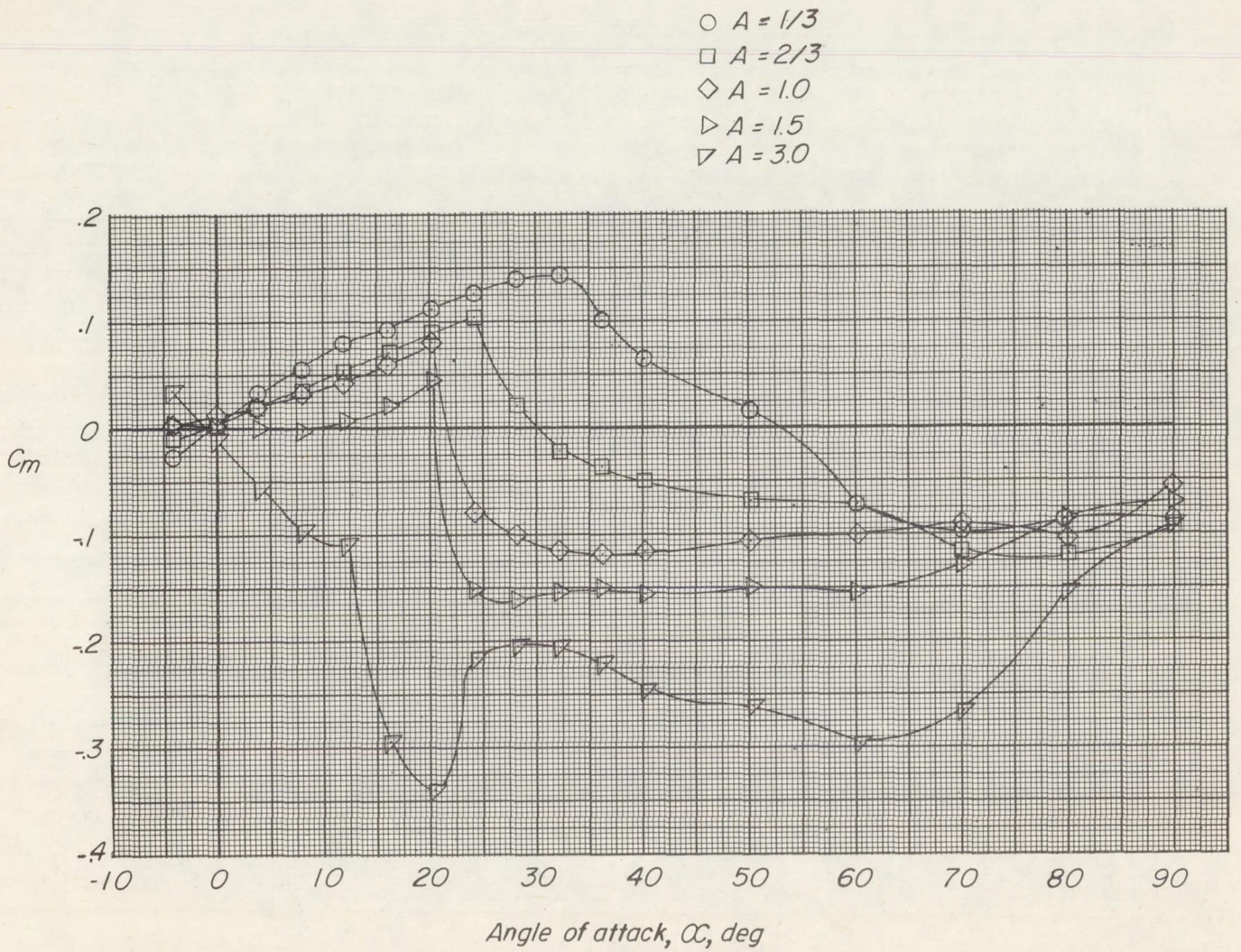

Figure 6.- Variation of pitching-moment coefficient with angle of attack for various aspect ratios.

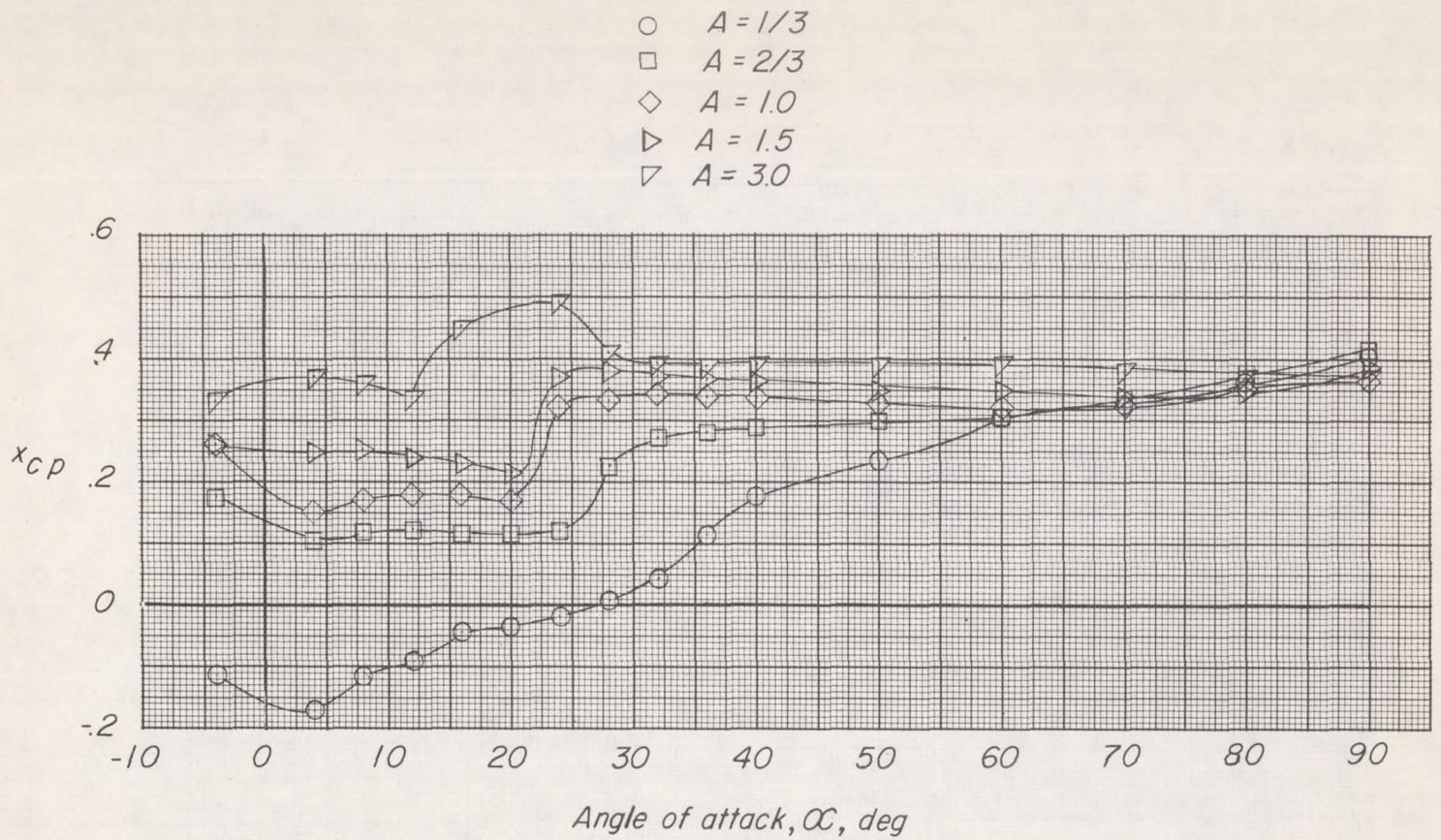

Figure 7.- Variation of center-of-pressure location with angle of attack for various aspect ratios.

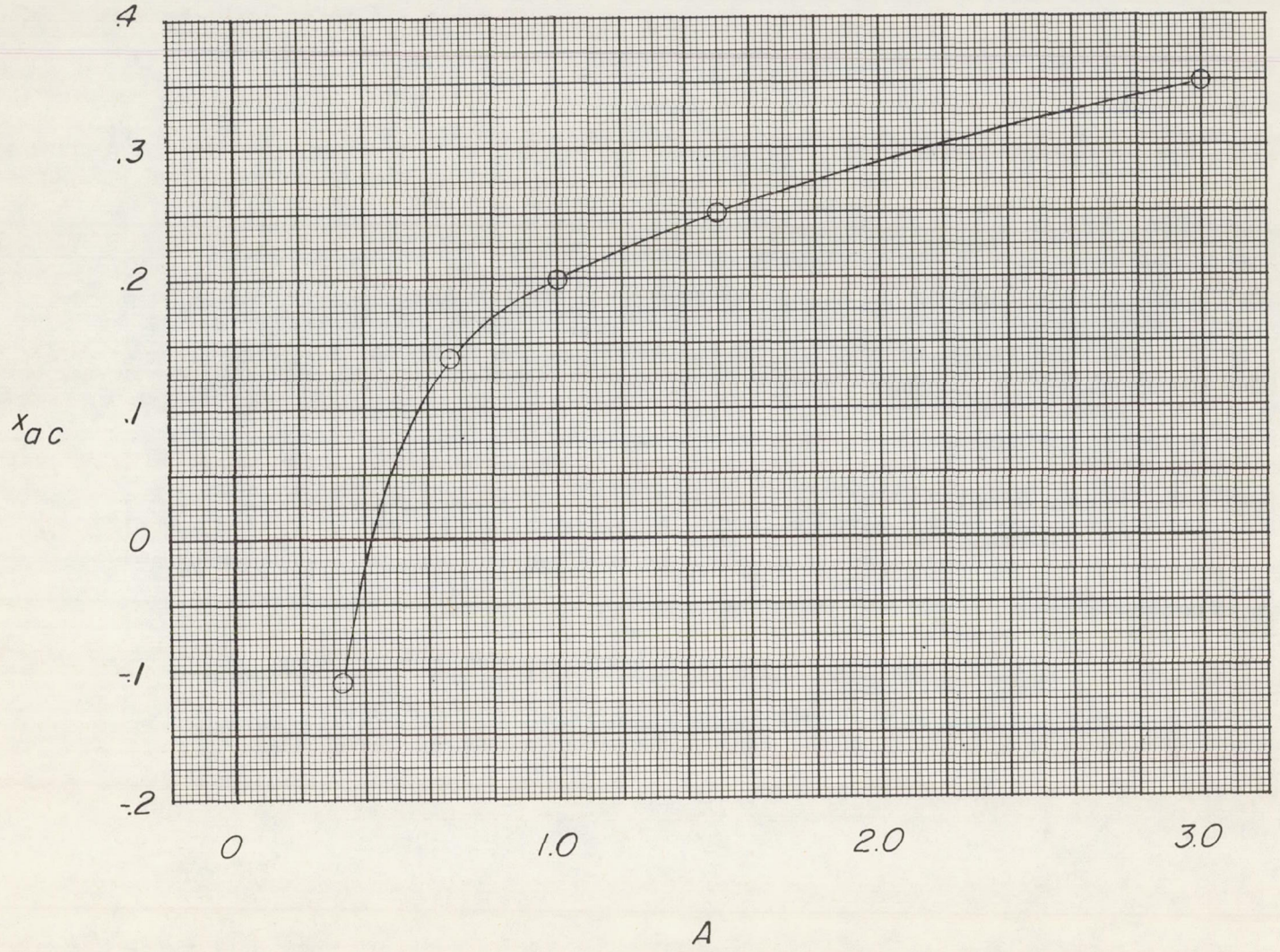

Figure 8.- Variation of aerodynamic-center location with aspect ratio.

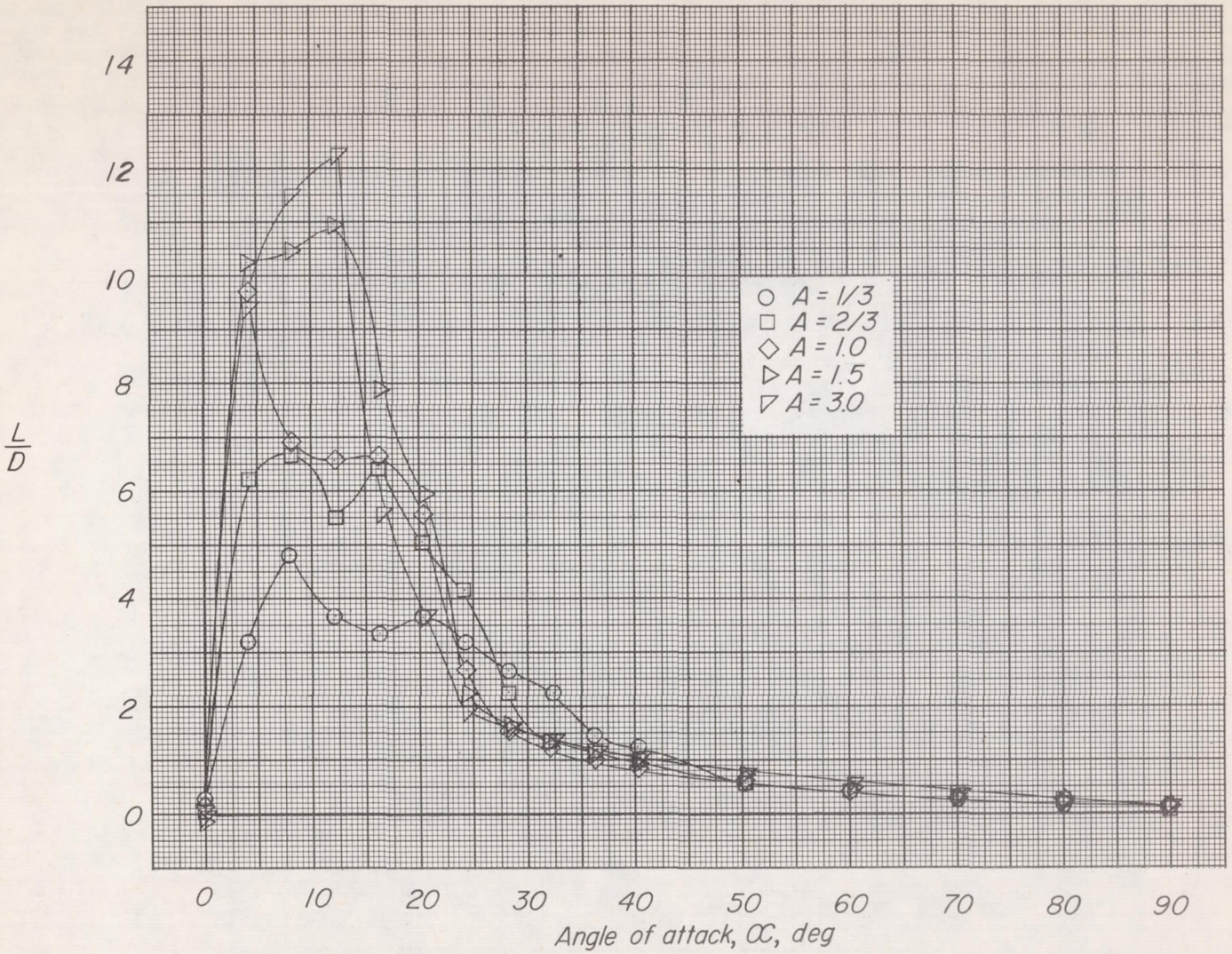

Figure 9.- Variation of lift-drag ratio with angle of attack for various aspect ratios.

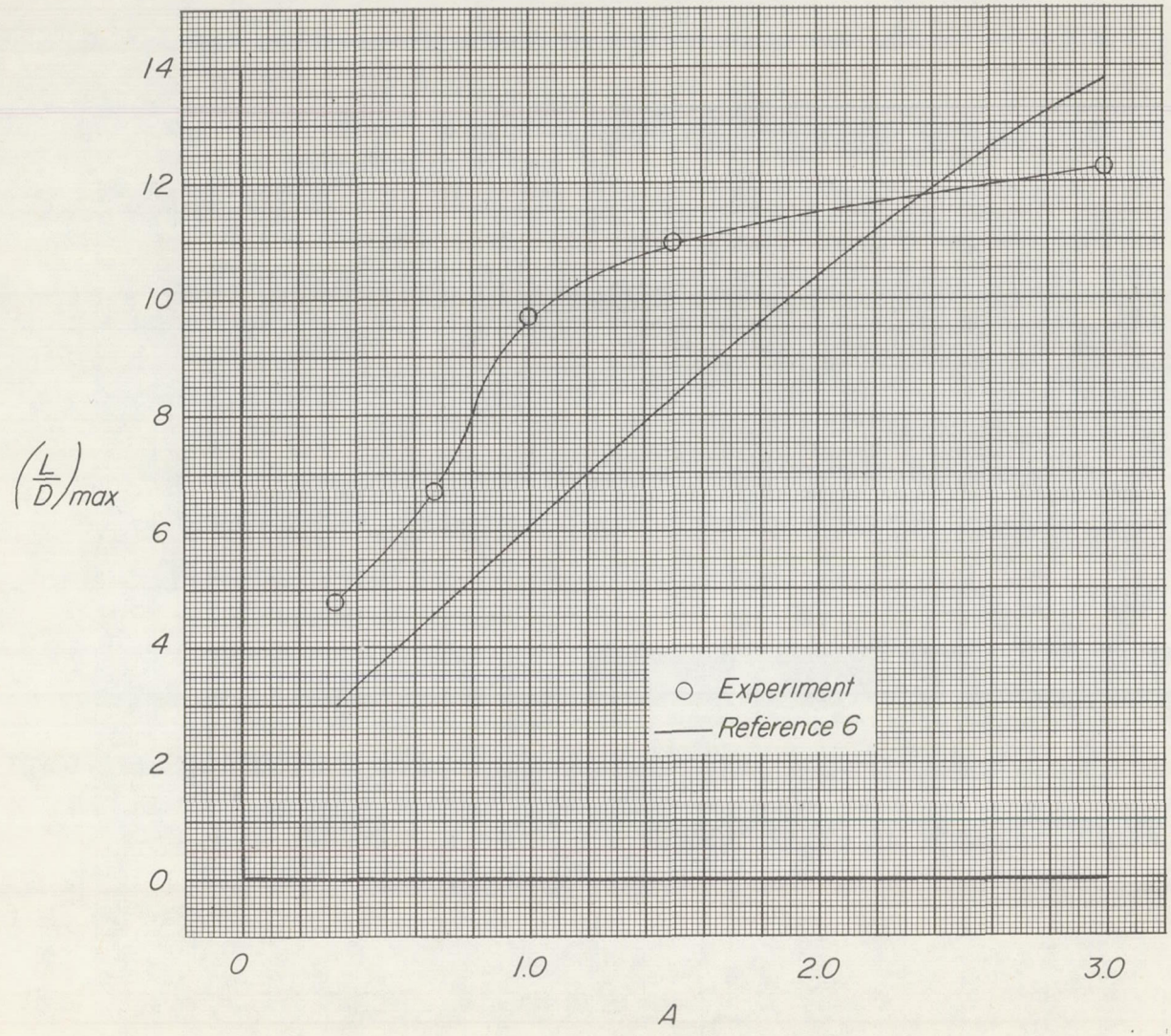

Figure 10.- Variation of maximum lift-drag ratio with aspect ratio.

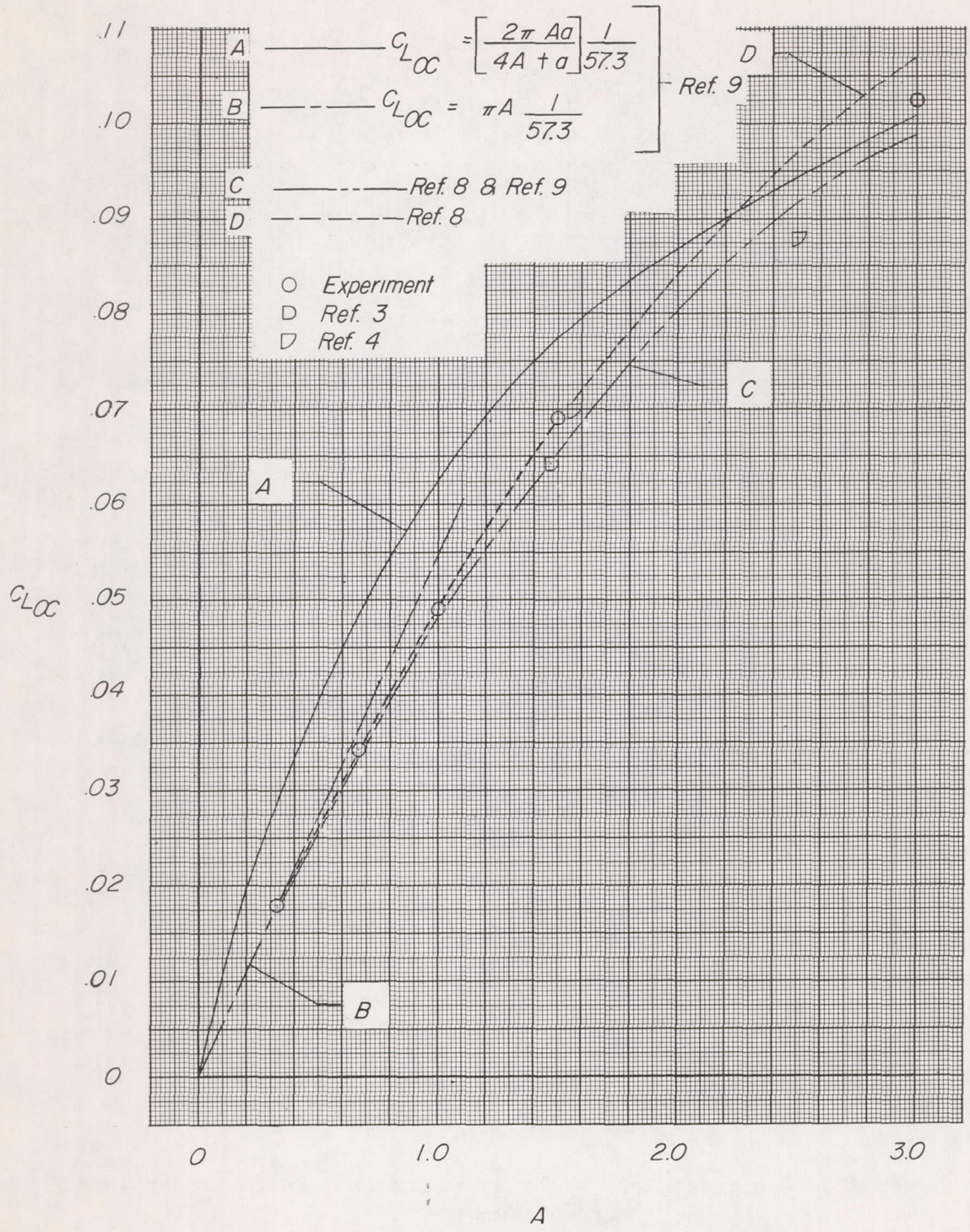

Figure 11.- Comparison of theoretical and experimental lift-curve slopes as function of aspect ratio.

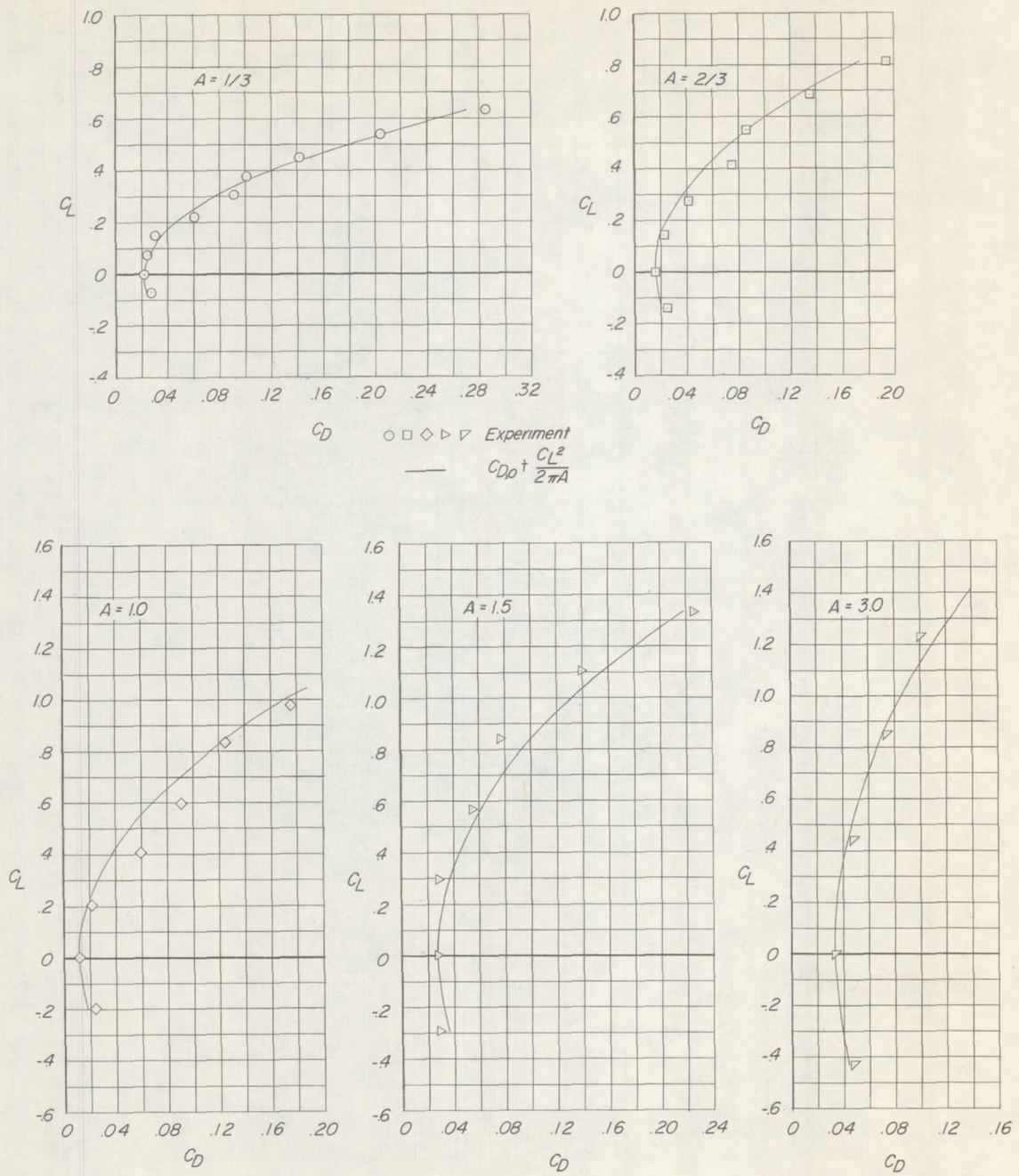

Figure 12.- Comparison of experimental and calculated drag polars for various aspect ratios.

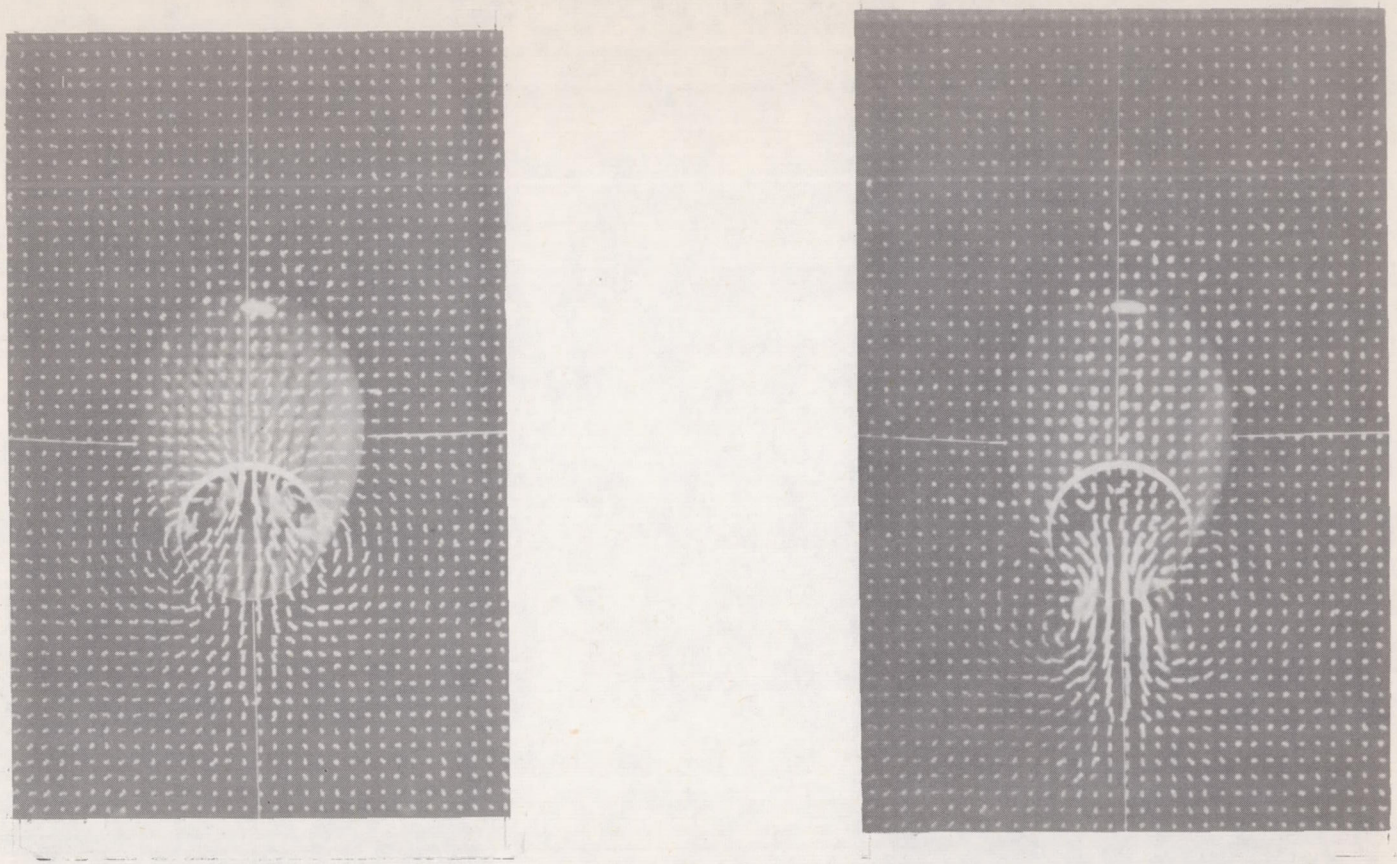

x = 3.5 x = 27.5

(a) A = 1/3; $\alpha = 19.5^{\circ}$. L-57-2708

Figure 13.- Tuft-grid photographs of flow behind various wings.

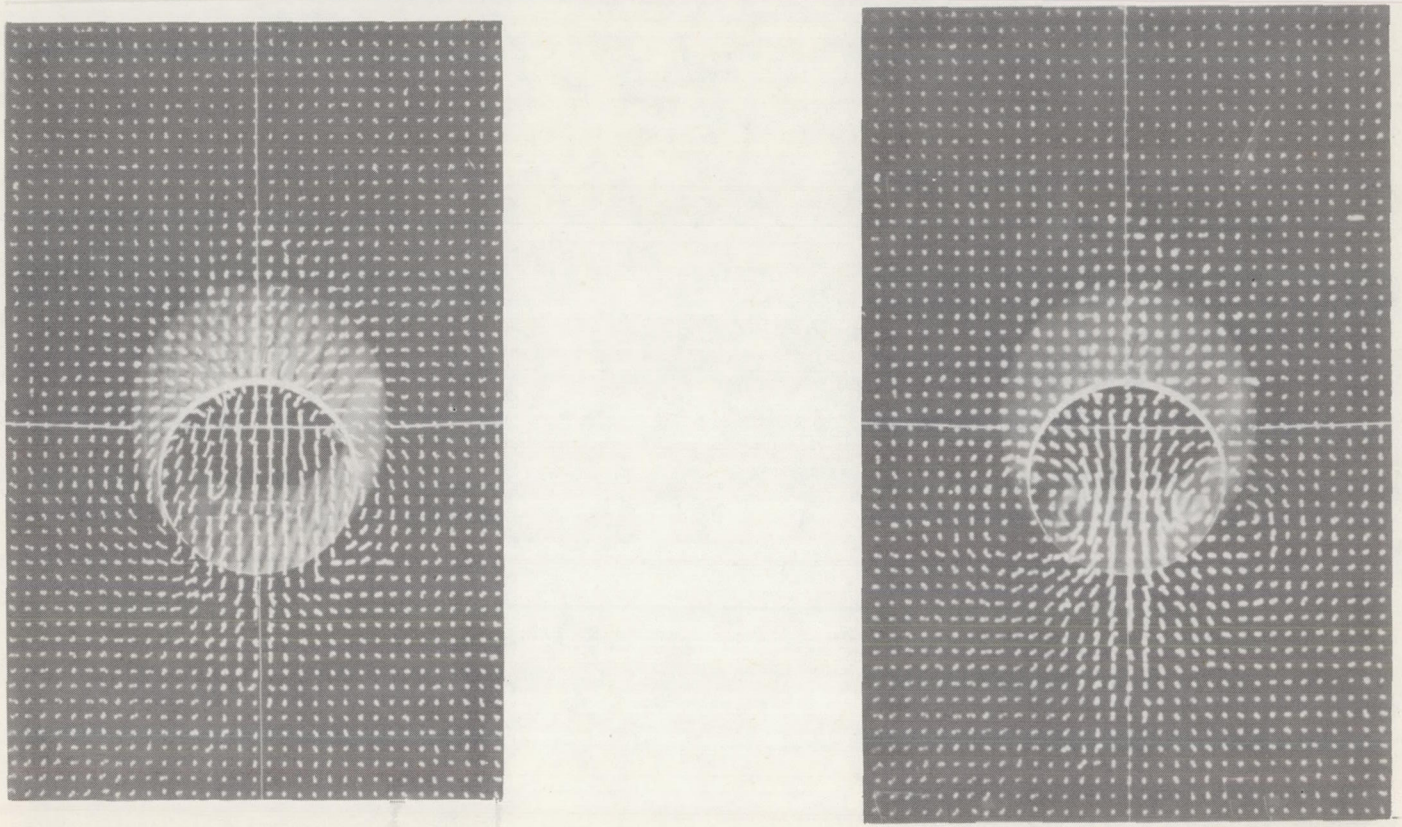

x = 1.5

x = 25.5

(b) A = 2/3; $\alpha = 20.1^{\circ}$. L-57-2709

Figure 13.- Continued.

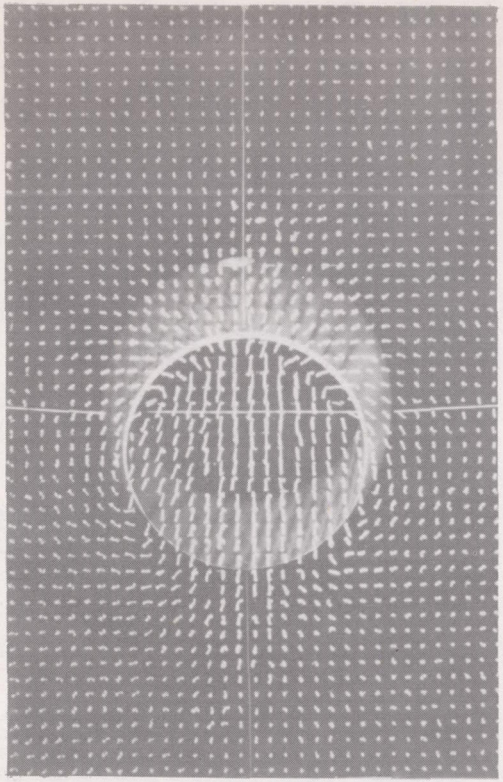

x = 3.125

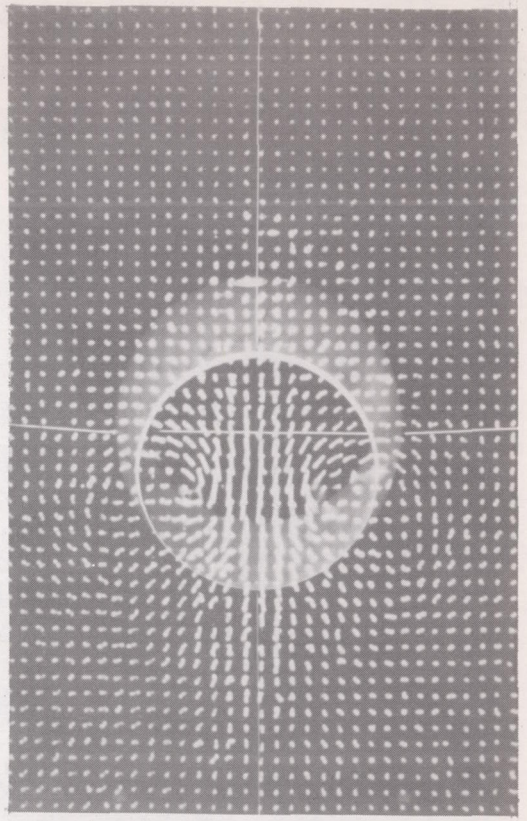

x = 27.125

(c) A = 1.0; $\alpha = 13.5^{\circ}$. L-57-2710

Figure 13.- Continued.

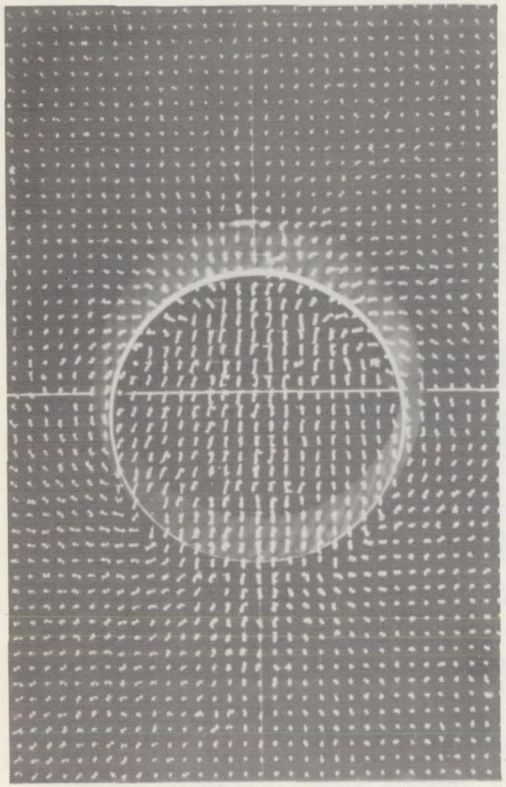

x = 6.0

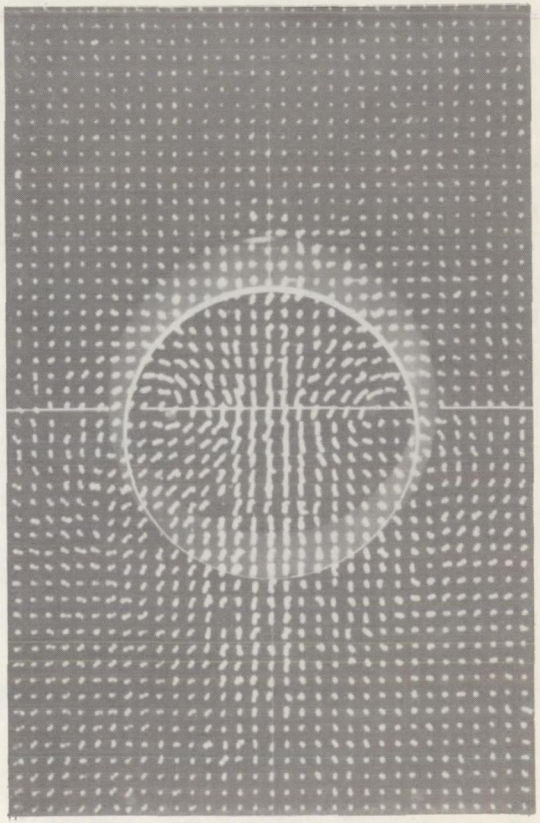

x = 30.0

(d) A = 1.5; $\alpha = 16.0^{\circ}$. L-57-2711

Figure 13.- Continued.

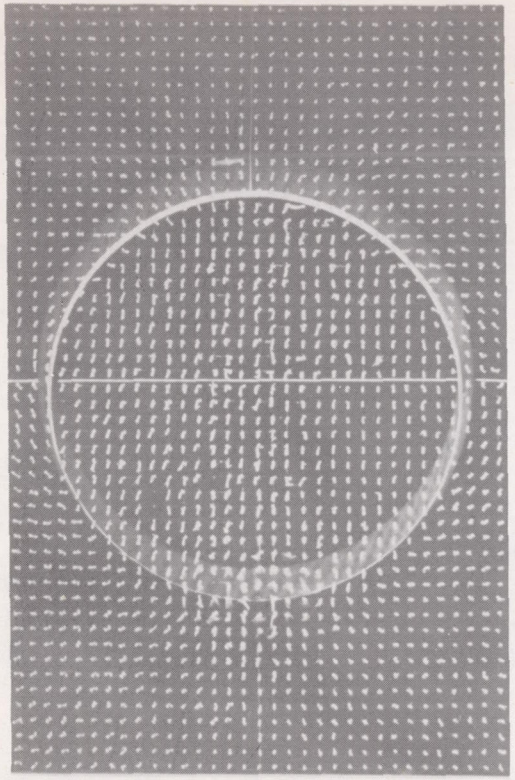

x = 4.125

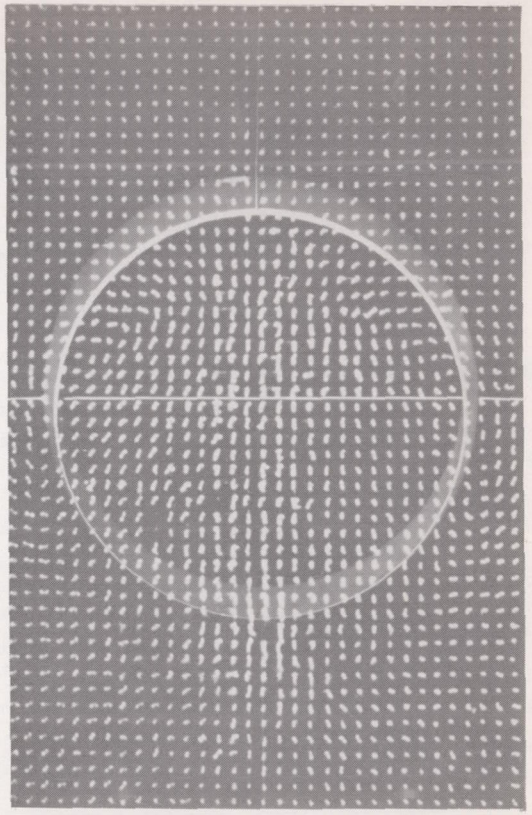

x = 28.125

(e) A = 3.0; $\alpha = 12.0^{\circ}$. L-57-2712

Figure 13.- Concluded.